Babeş-Bolyai University, Faculty of Environmental Science and Engineering, Cluj-Napoca

Temporal limitation of luminescence dating: on the saturation of the optically stimulated luminescence (OSL) signal of quartz

Doctoral Thesis Summary

Valentina Anechitei-Deacu

Promoters: Assoc. Prof. Dr. Alida Gabor (Timar)

Prof. Dr. Constantin Cosma

Cluj-Napoca 2018

The research discussed in the present thesis was mainly carried out at the Environmental Radioactivity and Nuclear Dating Centre, Interdisciplinary Research Institute on Bio-Nano-Science, Babeş-Bolyai University in Cluj-Napoca, Romania.

Valentina Anechitei-Deacu performed two research stages (about five months in total) at the Nordic Laboratory for Luminescence Dating (Denmark) and part of the work presented here was carried out during these stages.

Valentina Anechitei-Deacu benefited from financial support from:

The Romanian National Authority for Scientific Research CNCS-UEFISCDI through project PN-II-RU-TE-2011-3-0062.

The Sectorial Operational Programme for Human Resources Development 2007-2013, co-financed by the European Social Fund, under the project POSDRU/159/1.5/S/133391 – "Doctoral and postdoctoral excellence programs for training highly qualified human resources for research in the fields of Life Sciences, Environment and Earth".

The European Research Council (ERC) under the European Union's Horizon 2020 research and innovation programme ERC-2015-STG (grant agreement No [678106]).

Contents

Keywords: luminescence dating, optically stimulated luminescence (OSL); fine quartz; coarse quartz; single-aliquot regenerative dose (SAR) protocol; quartz dose response curve; natural signal; saturation; signal brightness.

Introduction

1.1. Introduction

Luminescence dating is part of the family of radiation damage dating methods alongside electron spin resonance (ESR) and fission track dating. The radiation damage is the result of mineral exposure to the ionising radiations coming from naturally occurring radionuclides and also from cosmic rays. The minerals, such as quartz and feldspar, have the ability to store the ionising radiation energy in the form of trapped charge that upon stimulation can result in a luminescence signal which can be quantified. If the charge is released by exposure to heat, the light emission is called thermoluminescence (TL) and if light is used to release the trapped charge, the light emission is called optically stimulated luminescence (OSL). The age is calculated by dividing the the paleodose (Gy) which is total dose received by minerals since the last zeroing event by the environmental dose rate (Gy/ka). In the case of sedimentary samples, the last zeroing event is represented by the exposure of minerals to daylight during erosion and transport and the dated event is the sediment deposition. The total dose received by minerals is determined in the laboratory as an equivalent dose based on the comparison of the natural OSL with the OSL signals induced by known doses given in the laboratory. At present, the single-aliquot regenerative-dose (SAR) procedure (Murray and Wintle, 2000; 2003) is the most frequently applied method for equivalent dose determination. The rate at which the dose was absorbed by the minerals can be calculated based on the specific activities of the radionuclides in the sediment, which can be determined by high-resolution gamma spectrometry or other methods. Loess and other windblown sediments are considered ideal materials for the application of luminescence dating, a powerful technique for dating late Quaternary deposits.

Despite the robustness of the SAR protocol (Wintle and Murray, 2006), an increasing number of studies have reported on SAR-OSL age underestimation for samples older than 40 ka (D_e values >~100-200 Gy) (see Murray et al., 2007; Buylaert et al., 2008; Lai, 2010; Lowick et al., 2010a). Additional problems have emerged when OSL studies were first applied to fine (4-11 μm) and coarse (usually 63-90 μm) quartz extracted from the same samples. The SAR-OSL ages obtained on the two quartz fractions extracted from loess from Romania, Serbia and China were reported to underestimate the true burial age, the fine fraction showing an earlier and more pronounced age underestimation (Timar et al., 2010; Timar-Gabor et al., 2011; Timar-Gabor et al., 2012; Timar-Gabor and Wintle, 2013; Constantin et al., 2014; Constantin et al., 2015; Timar-Gabor et al., 2015a; Timar-Gabor et al.,

2017). Moreover, the OSL ages and corresponding equivalent doses obtained on coarse (63-90 μm) quartz were reported to be systematically higher than those for the fine (4-11 μm) quartz for ages >~40 ka (D_e values >~100-200 Gy).

Different saturation characteristics were also reported for fine (4-11 μm) and coarse (63-90 μm) quartz extracted from loess, with the fine grains displaying much higher saturation characteristics (see Timar-Gabor et al., 2015b). Another important observation refers to the inconsistency between the natural and the laboratory-generated dose response curves (DRCs) for both fine (4-11 μm) and coarse (63-90 μm) quartz (Timar-Gabor et al., 2015b; Constantin et al., 2015). The growth of the signal in nature is described by a single saturating exponential function, whereas two such functions are needed to fit the laboratory dose response curves. The natural and laboratory DRCs start to diverge from each other above ~100-200 Gy and the laboratory-induced signal continues to grow at doses >300 Gy where the natural signal is seen in saturation. The divergence of the two DRC is more perceivable in the fine grains. Whereas the age discrepancy is thought to originate from the different saturation characteristics of fine (4-11 μm) compared to coarse (63-90 μm) quartz DRCs and from the different patterns of growth of the natural and laboratory DRCs, the mechanisms behind these experimental observations are not yet understood.

Part of the results presented in this thesis are part of a research project financed by the European Research Council (ERC) („INTERTRAP- Integrated dating approach for terrestrial records of past climate using trapped charge methods", StG 678106, HORIZON 2020) implemented in the Environmental Radioactivity and Nuclear Dating Centre of Babeș-Bolyai University in Cluj-Napoca. The main aim of the project is to investigate the mechanisms responsible for the controversial results obtained for Romanian, Serbian and Chinese loess (as described above) by the development of an integrated approach based on optically stimulated luminescence (OSL), thermoluminescence (TL) and electron spin resonance (ESR) investigations. The results presented in this thesis add to the first type of investigations, with emphasis on the issues related to the laboratory saturation of the OSL signal. Single-grain and multi-grain aliquot OSL data obtained for the high dose region of the SAR dose response curve are presented throughout the thesis, as described below.

1.2. Outline of the thesis

This thesis is structured in 4 main chapters. Chapters III and IV rely on articles I have authored (Anechitei-Deacu et al., 2018a and b). Chapters I and II contain some of the results published in articles I have co-authored (del Valle et al., 2016; Karátson et al., 2016; Timar-Gabor et al., 2017). Chapter 1 introduces the basic concepts in OSL dating. Chapter 2 is

mainly based on the study of literature and provides the basics necessary to understand the subsequent studies presented in this thesis. The problem of age and equivalent dose underestimation is discussed alongside other limitations reported when SAR-OSL dating was applied to fine (4-11 μm) and coarse (usually 63-90 μm) quartz. Chapter 3 present luminescence dating investigations on fine (4-11 μm) and different coarse (in the range 63-250 μm) fractions extracted from carbonate aeolianites at one site in SW Eivissa (Spain). The aim of this research is to gain more insights into the discrepant results previously reported for fine (4-11 μm) and coarse (63-90 μm) quartz extracted from loess (Timar-Gabor et al., 2017); Chapter 4 presents single and multi-grain single aliquot regenerative (SAR) OSL investigations for a coarse-grained (180-250 μm) quartz sample extracted from loess collected below the Brunhes/Matuyama transition at the Roksolanyloess profile in Ukraine. The aim is to investigate the degree of correspondence between the natural OSL signal and the SAR laboratory saturation level for an 'infinitely' old sample (from the perspective of OSL dating using quartz). At the end of the thesis conclusions are being summarised.

1 Basic concepts in optically stimulated luminescence (OSL) dating

Optically stimulated luminescence (OSL) dating involves the use of light of a specific wavelength (usually in the visible range of the electromagnetic spectrum) for signal stimulation and a luminescence signal measured at a shorter wavelength. The OSL dating technique was development and first applied to quartz from sedimentary samples by Huntley et al. (1985) and is at present the method of choice for obtaining depositional ages for a large variety of sediments.

1.1. Principles of optically stimulated luminescence dating

The moment that is dated using luminescence is the last exposure of sediment grains to daylight ("zeroing event"). The absorption of ionising radiation (from ^{238}U, ^{232}Th, their daughters and ^{40}K, and also from cosmic radiation) by the minerals results in the creation of free charges (electrons and holes) within the crystalline structure of the mineral, some of which may get trapped in certain defects within the crystal, leading to the build-up of luminescence signal. When exposed to daylight, the trapped electrons absorb enough energy in order to get detrapped and thus to reset the luminescence signal to zero. If the signal accumulated by the minerals from the last "zeroing event" is removed in the laboratory by exposure to light, it allows the luminescence signal to be measured and an estimate of the radiation dose absorbed during the burial period to be determined as an equivalent dose (D_e).

When both the equivalent dose and the dose rate are determined, the luminescence age can be calculated using the following formula:

$$Age\ (ka) = \frac{equivalent\ dose\ (Gy)}{annual\ dose\ (\frac{Gy}{ka})} \tag{1.1}$$

1.2. Mechanism of optically stimulated luminescence

The simplest model used to explain the process of optically stimulated luminescence production in quartz (Aitken, 1998) is based on one trap and one recombination centre configuration. During the interaction of the crystal with the ionising radiation, the electrons from the valence band receive enough energy to make the transition from this band to the conduction band. When this happens, there is a lack of an electron (defined as a hole) left in the valence band. The holes may get trapped at defects with negative charge and behave as recombination centres. As the electrons can not be accumulated in the conduction band, they will either return to the valence band or will get trapped at defects in the band gap. By

exposing the crystal to energy, trapped electrons escape into the conduction band, from where a fraction will get retraped and the rest will recombine with the trapped holes at the recombination centres. If the recombination centre is radiative, a photon will be emitted. If the stimulating energy is in the form of light, the emission is called optically stimulated luminescence (OSL).

1.3. The single-aliquot regenerative-dose protocol (SAR)

A typical single-aliquot regenerative-dose (SAR) measurement protocol (Murray and Wintle, 2000, 2003; Wintle and Murray, 2006) is outlined in **Table 1.1**. A dose response curve is constructed for a quartz aliquot using the sensitivity-corrected OSL signals (L_x/T_x) obtained for different laboratory given regenerative doses. The equivalen dose (D_e) is determined by interpolating the natural sensitivity-corrected signal (L_n/T_n) on this dose response curve.

Table 1.1. Generalised SAR sequence for quartz.

Step	Treatment
1	Give dose (D_i)[a]
2	Preheat (160-300 ºC for 10 s)
3	Optically stimulate[b] for x seconds at 125 ºC (**L_x**)
4	Give test dose (D_t)
5	Heat to T < preheat temperature in step to (cutheat)
6	Optically stimulate for x seconds at 125 ºC (**T_x**)
7	Optically stimulate for 40 s at T > preheat in step 2
8	Return to step 1

[a] During the first SAR cycle, when the natural dose is measured, i = n and D_n = 0 Gy.

[b] The stimulation time vary as function of stimulation light intensity and wavelength.

There are several tests used to evaluate the performance of the SAR protocol, i.e. recycling, recuperation, preheat plateau and dose recovery tests. The recycling test checks whether the sensitivity changes are accurately corrected throughout the SAR cycles. The recuperation test examines whether the thermal transfer of charge from one SAR cycle to the next is significant. A preheat test can be used to assess the influence of preheat temperature on D_e estimates, by plotting the D_e values as function of preheat temperature. The most rigorous test for evaluating the performance of the SAR protocol is the dose recovery test which examines the ability of the SAR protocol to accurately recover a known dose given in

the laboratory. The contamination of the quartz extract with feldspars is checked by using the infrared stimulated luminescence (IRSL) response to a large regenerative β-dose measured at 60 °C (IR depletion test; Duller, 2003)

1.4. Sample preparation

Sample preparation for luminescence investigations is performed in the laboratory under low intensity red light, to avoid bleaching of the quartz luminescence signal. Conventional procedures for quartz extraction (Aitken, 1985; Lang et al., 1996; Frechen et al., 1996) include treatments with different acids, sieving steps, density separation, separation based on Stokes's law and centrifugation in distilled water.

1.5. Instrumentation

All optically stimulated luminescence (OSL) measurements were carried out using automated TL/OSL Risø DA-20 readers (Bøtter-Jensen et al., 2010).

2 Reliability of the single-aliquot regenerative-dose (SAR) protocol

2.1. Introduction

The development of the single-aliquot regenerative-dose (SAR) protocol (Wintle and Murray, 2000) almost two decades ago has revolutionised luminescence dating by giving rise to high precision equivalent dose (D_e) estimates, commonly with standard errors of <5%. However, for samples lacking independent age control, the accuracy of the OSL ages remains questionable despite the good performance of the quartz samples in the SAR protocol.

2.2. Validation of the OSL ages

There are a number of dating methods which overlap the age range covered by luminescence dating techniques. However, validation of the OSL ages by independent age control is hindered by the lack of methods which can directly date the depositional time of the sediments. Chronological control is also provided by the repeated glacial-interglacial cycles recorded in global paleoclimatic archives for which a timescale was established by correlating proxy-climate records to orbital periodicities, process known as orbital tuning. For loess-paleosol deposits, which are extensively dated by luminescence techniques, identification of the paleosol associated with Marine Istope Stage (MIS) 5 (71-130 ka; Lisiecki and Raymo, 2005) is known to provide valuable time control. The identification of the last interglacial paleosol provides a minimum age threshold for the sediments underlying it, which should be no younger than ~130 ka.

2.2.1. Studies reporting agreement between OSL ages and independent age control

There are several studies reporting agreement up to and even beyond the last interglacial (the Eemian, lasting from ~130 to ~116 ka; Shackleton (2000)) between quartz OSL ages obtained using the SAR protocol and independent age control (see for example Murray and Olley, 2002; Murray et al., 2008; Pawley et al., 2008).

2.3. The problem of age underestimation

2.3.1. Saturation characteristics of the OSL signal

The maximum limit for dating using the fast-component OSL signal from quartz (the initial part of the signal is referred to as the fast component) is given by the dose at which the signal reaches saturation. Additionally, the upper age limit varies with the magnitude of the environmental dose rate, the OSL chronologies obtained for low dose rate sediments extending further back in time.

Assuming that a single electron trap/ recombination centre is responsible for the optically stimulated luminescence production in quartz, the growth of the OSL signal with dose is expected to be described by a single saturating exponential function (Aitken, 1998**)** (Eq. (2.1)). Such dose response curves were obtained using the fast component of coarse (>63 µm) quartz and D_0 values ranging between 55 and 190 Gy were reported (see Wintle and Murray, 2006). In this case, an upper limit of 2 x D_0 is recommended for deriving reliable equivalent doses (Wintle and Murray, 2006). The 2 x D_0 limit is equivalent to 86% of the saturation level, as results from substituting *D* for $2D_0$ in Eq. 2.1. D_e values derived beyond this limit will be affected by large and asymmetric uncertainties.

$$I(D) = I_0*(1-\exp(-D/D_0)) \quad (2.1)$$

where *I* is the OSL signal measured for a dose D, I_0 is the maximum OSL intensity and D_0 is the dose that characterise the curvature of the dose response curve (also named characteristic dose).

However, many studies published over the past years have reported on the need of an additional component to describe the growth of the OSL signal at high doses (>~100 Gy). Although initially reported as an additional linear term (Roberts and Duller, 2004, Li et al., 2015, Buylaert et al., 2008, Timar et al., 2010), it was shown to represent the early expression of a second saturating exponential function (Lowick et al., 2010b).

2.3.2. Reliability of the equivalent doses derived from quartz samples displaying dose response curves (DRCs) with more than one component.

The presence of a second component in the high-dose response (>100 Gy) of quartz OSL is not yet fully understood. Quartz OSL displaying a continuing growth at high doses should theoretically allow to obtain higher equivalent doses; however, it has been suggested that the D_e values derived from this region should be treated with caution when comparison with independent age control is not possible, as many studies reported on age underestimation for equivalent doses >100-200 Gy (see for example Murray et al., 2007; Lai, 2010; Lowick et al., 2010a, Lowick and Preusser, 2011).

2.3.3. Importance of grain size - identification of additional problems when using two grain sizes

The choice of the quartz grain size is usually related to the dominant grain size within the investigated sedimentary unit and it is common practice to use only one fraction for investigations. However, when two grain sizes (4-11 and 63-90 µm) of quartz have been extracted from loess sites in south-eastern Europe and China, a series of controversies were reported (see Timar-Gabor et al., 2017). These include an earlier and more pronounced age underestimation for the fine (4-11 µm) compared to the coarse (63-90 µm) quartz fraction as well as systematically higher OSL ages and corresponding equivalent doses for coarse quartz than those for the fine quartz for ages >~40 ka (D_e values >~100-200 Gy) (Timar et al., 2010; Timar-Gabor et al., 2011; Timar-Gabor et al., 2012; Timar-Gabor and Wintle, 2013; Constantin et al., 2014; Constantin et al., 2015; Timar-Gabor et al., 2015a; Timar-Gabor et al., 2017). The lower equivalent doses measured on fine grains compared to the coarse fraction are thought to result from the combined effect of two issues. Firstly, the interpolation of the corrected natural luminescence signal for the two fractions on SAR dose response curves (DRCs) that for doses higher than ~100 Gy start to deviate from each other, with the response curve for fine quartz growing to much higher doses (see **Fig. 2.1**); then, the fact that the laboratory DRCs grow to higher doses than the natural DRCs, with a more pronounced difference in the case of the fine fraction.

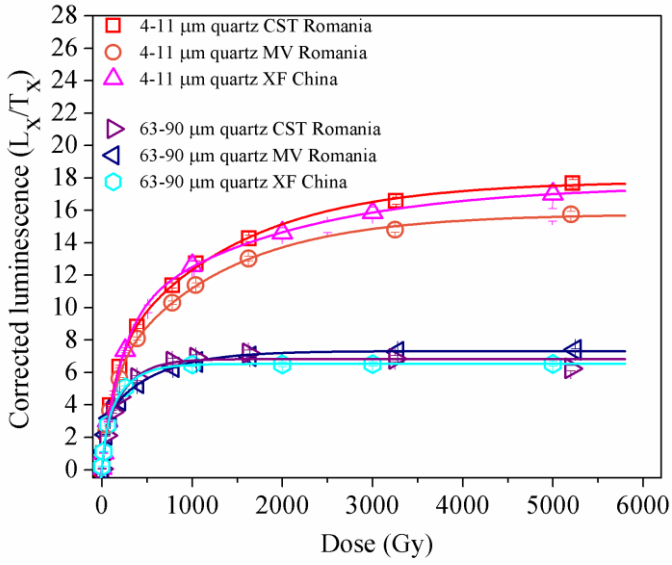

Fig. 2.1. Representative SAR dose response curves for fine (4-11 µm) and coarse (63-90 µm) quartz extracted from Romanian and Chinese loess. From Timar-Gabor et al. (2017) (the logarithmic scale was changed to linear**)**.

2.4. Conclusions

The SAR protocol is the most robust and precise procedure currently available for equivalent dose estimation. However, various SAR-OSL studies conducted during the past years on quartz of different grain sizes and from diferent geological contexts have reported underestimation for ages higher than 40 ka and corresponding equivalent doses >100-200 Gy. Moreover, SAR-OSL investigation using fine (4-11 μm) and coarse (63-90 μm) quartz fractions from loess samples resulted in additional problems, including different saturation characteristics of the dose response curves of the two fractions, a different growth pattern of the natural dose response curve relative to the laboratory-generated dose response curve for both quartz fractions and the consequential age discrepancies between fine and coarse quartz, and more pronounced age underestimation for fine quartz. The mechanisms behind these issues remain as yet unknown, despite the increasing number of studies aimed at gaining insights into these observations.

3 Assessing the maximum limit of SAR-OSL dating using quartz of different grain sizes – based on Anechitei-Deacu et al. (2018a)

3.1. Introduction

This study was aimed at gaining gain further insight into the possible processes that might be involved in giving rise to the discrepant results obtained for fine and coarse quartz extracted from Romanian, Serbian and Chinese loess samples, by investigating samples containing quartz with a different geological origin, from a different depositional environment and which are expected to have annual dose rates lower than those for loess, namely less than 1 Gy/ka (Fornós et al., 2009). Measurements have been made on fine (4-11 μm) and coarse (63-90, 90-125, 125-180 and 180-250 μm) grains extracted from carbonate-rich aeolianites from one site on Eivissa (Balearic Islands); we also compare the luminescence properties of the quartz extracted from these samples with those of quartz separates from our previously investigated samples of Chinese loess from Xifeng loess-paleosol section (Timar-Gabor et al., 2017).

3.2. Material and methods

3.2.1. Study area

The island of Eivissa is the third largest (571 km^2) and the most western island of the Balearic Archipelago and is located in the southwestern part of the Mediterranean Sea. The coastal section at Cala Bassa, located in the southwest of the island has been investigated in this study.

3.2.2. Samples and analytical facilities

The three aeolianite samples collected at Cala Bassa were processed to extract fine (4-11 μm) and four different coarse fractions (63-90 μm, 90-125 μm, 125-180 μm and 180-250 μm). All luminescence measurements were undertaken using a Risø TL/OSL-DA-20 reader (Bøtter-Jensen et al., 2010). Annual dose rate determination was based on high-resolution gamma spectrometry measurements; the information relevant for annual dose estimation is given in **Table 3.1**.

Table 3.1. Equivalent doses (D_e), dosimetry measurements and OSL ages. The luminescence and dosimetry data are indicated along with the random uncertainties; the uncertainties mentioned with the OSL ages are the overall uncertainties. All the errors correspond to 1σ.

Sample code	Grain size (μm)	Water content (%)	D_e (Gy)	U-Ra (Bq/kg)	Th (Bq/kg)	K (Bq/kg)	Total random error (%)	Total systematic error (%)	Total dose rate (Gy/ka)	Age (ka)	Weighted average age (ka)
M#11#	4-11	4	133±2 $_{n=8}$	16.2±0.7	2.0±0.6	19.3±3.5	3.4	9.9	0.73±0.02	182±19	172±12
	63-90		107±4 $_{n=8}$				4.8	6.2	0.61±0.02	176±14	
	90-125		103±5 $_{n=11}$				5.7	6.3	0.60±0.02	172±15	
	125-180		107±6 $_{n=10}$				6.3	6.3	0.59±0.02	180±16	
	180-250		91±5 $_{n=11}$				6.2	6.3	0.59±0.02	154±14	
M#6#	4-11	4	175±2 $_{n=8}$	16.0±0.6	2.0±0.5	54.9±3.0	2.6	9.0	0.80±0.02	220±21	236±15
	63-90		165±4 $_{n=10}$				3.3	5.7	0.67±0.02	247±16	
	90-125		155±9 $_{n=9}$				6.2	5.7	0.66±0.01	237±20	
	125-180		175±7 $_{n=10}$				4.6	5.7	0.65±0.01	270±20	
	180-250		137±6 $_{n=8}$				4.9	5.7	0.65±0.01	212±16	
M#9#	4-11	2	179±2 $_{n=8}$	16.5.±0.2	2.7±0.5	24.2±3.1	2.4	10.1	0.73±0.02	244±25	250±16
	63-90		139±6 $_{n=12}$				4.8	5.7	0.60±0.01	232±17	
	90-125		146±5$_{n=10}$				4.0	5.7	0.59±0.01	248+17	
	125-180		148±5 $_{n=10}$				4.0	5.7	0.58±0.01	253±18	
	180-250		161±7 $_{n=10}$				4.8	5.7	0.58±0.01	277±21	

n denotes the number of accepted aliquots.

Radionuclide concentrations were derived by high-resolution gamma spectrometry and were converted to dose rates using published conversion factors (Adamiec and Aitken, 1998).

The cosmic ray contribution was estimated using published formulae (Prescott and Hutton, 1994).

Water content estimation was based on the difference between the as found and the oven-dried weight of the sample. A time-averaged water content was derived for each sample with a relative error of 25%.

Beta attenuation and etching factor for 63-90 μm, 90-125 μm, 125-180 μm, 180-250 μm assumed to be 0.94 ± 0.047, 0.90 ± 0.045, 0.88 ± 0.044, 0.87 ± 0.044, respectively; adopted alpha efficiency factor was 0.04± 0.02.

The total dose rates include the contribution from alpha, beta and gamma radiations, and the contribution from the cosmic rays; an internal contribution 0.01Gy/ka was assumed for the coarse fraction. (Vandenberghe et al., 2008).

3.3. Results

3.3.1. General behaviour in the SAR protocol

The OSL signals from these samples (both fine and coarse) displayed a rapid decay during optical stimulation, being almost identical to that obtained for the calibration quartz measured using the same equipment. Linearly modulated (LM) OSL signals were also examined, confirming that the OSL signals from these samples are dominated by a fast component.

Luminescence investigations were performed using the SAR protocol (Murray and Wintle, 2000). In terms of the routine tests for the SAR protocol, very few aliquots (less than 5%) have been rejected based on the recycling ratio test; no aliquot has been eliminated due to contamination with feldspars and recuperation has not exceeded 0.4% of the natural signal. Preheat plateau and dose recovery tests were also applied to fine (4-11 μm) and coarse (63-90 μm) quartz grains from these samples.

3.3.1.1. Thermal stability of the OSL signal

To test the thermal stability of the OSL signal measured from 0 to 0.308 s, annealing curves were constructed, increasing the 10 s preheat in steps of 10˚C. The first order derivative of the curves shows the origin of the fast OSL signals for the 4-11 μm and 63-90 μm quartz from sample M#6# to be linked to a trap which has its maximum rate of emptying at a temperature of at least 300˚C. To further test the thermal stability of the OSL signal for quartz from these samples, an isothermal luminescence decay experiment was carried out for sample M#11# (63-90 μm), as described by Timar-Gabor et al. (2017). Our results show a trap lifetime of about 69 Ma at 20^{o}C, thus indicating that thermal instability is not an issue for quartz extracted from these samples and that the signal should be stable enough to date the last 1 Ma.

3.3.2. Equivalent doses and OSL ages

Equivalent doses were obtained using the SAR protocol on between 8 and 12 aliquots for both fine and coarse grains. The average D_e values obtained using the SAR protocol and the OSL ages are presented in **Table 3.1**. Agreement was obtained within error limits between the ages on the different quartz fractions and a weighted mean age was calculated for each sample (Aitken, 1985) (**Table 3.1**). An age of 172 ± 12 ka was found for the uppermost sample, and ages of 236 ± 15 ka and 250 ± 16 ka were found for two deeper units, 4-5 m apart. The good agreement for the ages on this timescale for the fine and coarse grain sizes is in stark contrast to the results obtained for loess from eastern Europe (see **Section 1.1**). However, it is important to note that the equivalent doses are fairly low (<200 Gy), due to the low dose rates which are characteristic of quartz from aeolianites.

3.3.3. Laboratory dose-response curves for high doses

As discussed in **Section 1.1**, the non-agreement of the ages for fine and coarse grains from loess may be the result of the different dose response curves encountered at higher doses. In this study, dose response curves have been constructed up to 2000 Gy for the five grain sizes extracted from the aeolianite sample M#6# (**Fig. 3.1**). Curve fitting was carried out using two saturating exponential functions of the form:

$$I(D) = I_0 + A*(1 - \exp(-D/D_{01})) + B*(1 - \exp(-D/D_{02})) \quad (3.1)$$

where I - intensity of the OSL signal corresponding to a dose, D; I_0 - residual luminescence signal; A, B - amplitude of the two exponential components; D_{01}, D_{02} – doses that characterise the curvature of the dose response curve.

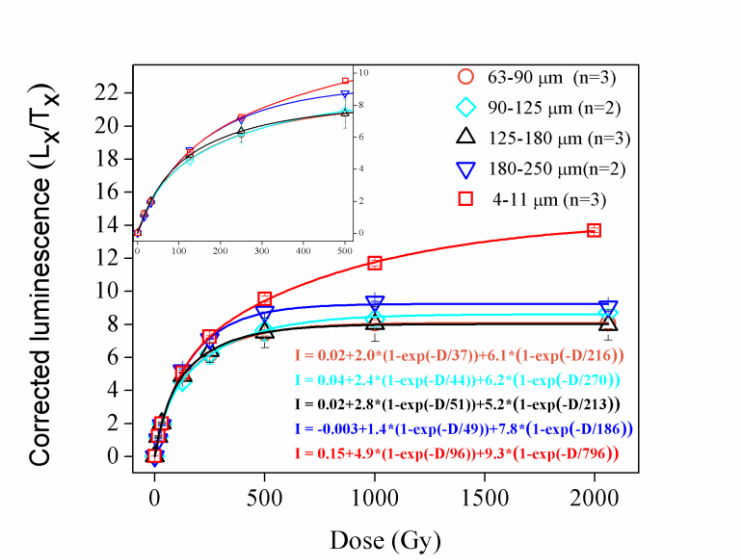

Fig. 3.1. SAR dose response curves for doses up to 2000 Gy for aliquots of 4-11, 63-90, 90-125, 125-180 and 180-250 µm quartz extracted from sample M#6#. The inset shows an enlargement for the dose region up to 500 Gy. The number of aliquots used for each fraction and the equations used to fit the curves are also indicated.

A very different growth pattern was observed for the fine and coarse quartz fractions. The regenerated luminescence signal for the coarse quartz grains reaches 86% of saturation level (equivalent to the 2 x D_0 limit for a single saturating exponential growth) (Wintle and Murray, 2006) for doses of ~350 Gy, whereas for the 4–11 µm quartz the regenerated signals attain ~86%

of saturation for doses of ~2000 Gy. Thus, the dose response behaviour for the aeolianite appears to be similar to that seen for the loess in eastern Europe and China (Timar-Gabor et al., 2017).

As seen in **Fig. 3.1**, the OSL signal of the fine fraction is not in saturation at 2000 Gy; thus, a dose response curve for fine quartz from sample M#6# was constructed up to 6000 Gy (**Fig. 3.2**). The values for D_{01} and D_{02} calculated from this data set are about double the values calculated when the maximum dose was 2 kGy (**Fig. 3.1**). Using the data in **Fig. 3.2**, but restricting the range of doses used for fitting to the first eleven doses, and then adding in one more data point in subsequent analyses, enables examination of the effect of the choice of the maximum dose point on calculation of D_{01} and D_{02} (**Fig. 3.3**). This clearly exemplifies the need to construct dose response curves up to full saturation in order to obtain meaningful values for the D_{01} and D_{02} parameters. Considering the error limits and the uncertainties of fitting using a restricted number of data points, the responses of the fine and coarse grains can be superimposed for doses up to ~200 Gy (inset to **Fig. 3.1**); it is for this dose region that values of D_e were obtained for these samples, resulting in similar ages for both fine and coarse grain sizes.

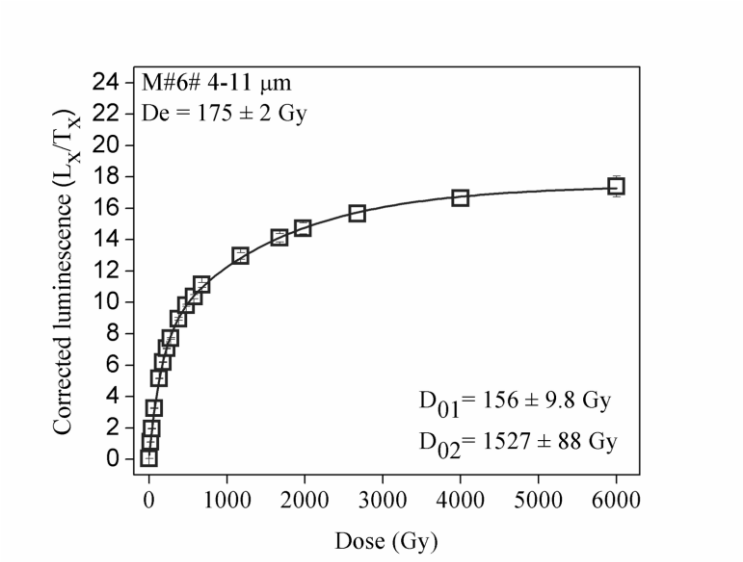

Fig. 3.2. Average SAR dose response curve for doses up to 6000 Gy for 3 aliquots of 4-11 μm from M#6#.

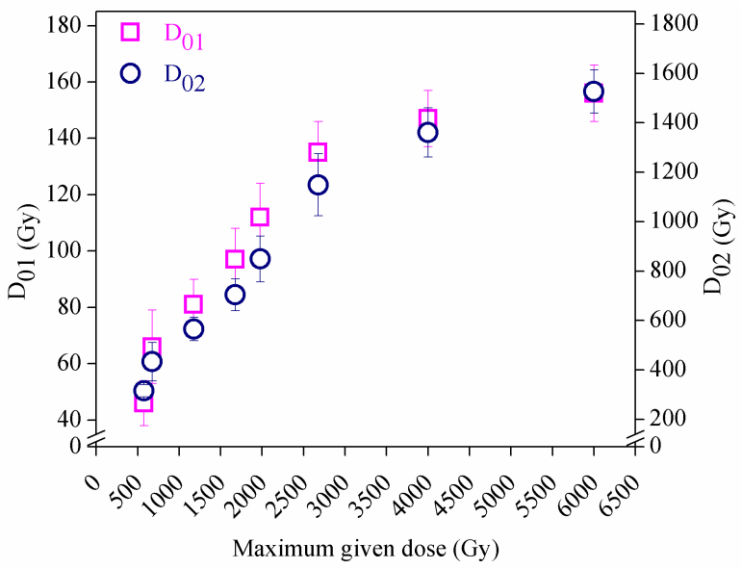

Fig. 3.3. Saturation characteristics (D_{01}, D_{02}) obtained from the data in **Fig. 3.2**, calculated when using increasingly high doses.

3.3.4. Adding laboratory doses before measurement

3.3.4.1. Quartz from aeolianites

As seen in **Fig. 3.1**, the SAR dose response curves for the various coarse grain fractions of sample M#6# reach the saturation level when doses of 1000 Gy are applied. This implies that if a dose of this order, e.g. 1500 Gy, is given in addition to the natural dose, the value of the sensitivity corrected signal, denoted by L_n*/T_n*, should also be at the same saturation level. This is not the case of the dose response curves for the fine quartz fraction which are close to saturation when doses up to 6000 Gy are given (**Fig. 3.2**). Aliquots of 4-11 μm quartz from sample M#6# (D_e = 175 ± 2 Gy) were given 1500 Gy on top of the natural dose (**Fig. 3.4a**); the response intersects the subsequently constructed dose response curve enabling an apparent equivalent dose to be measured (1040 ± 35 Gy), thus giving a value that is less than the known dose that was given. This behaviour contrasts with the results for the 63-90 μm grains from this sample where the response to the natural plus added dose is at the same level as the saturation level of the subsequently measured SAR dose response curve (**Fig. 3.4b**).

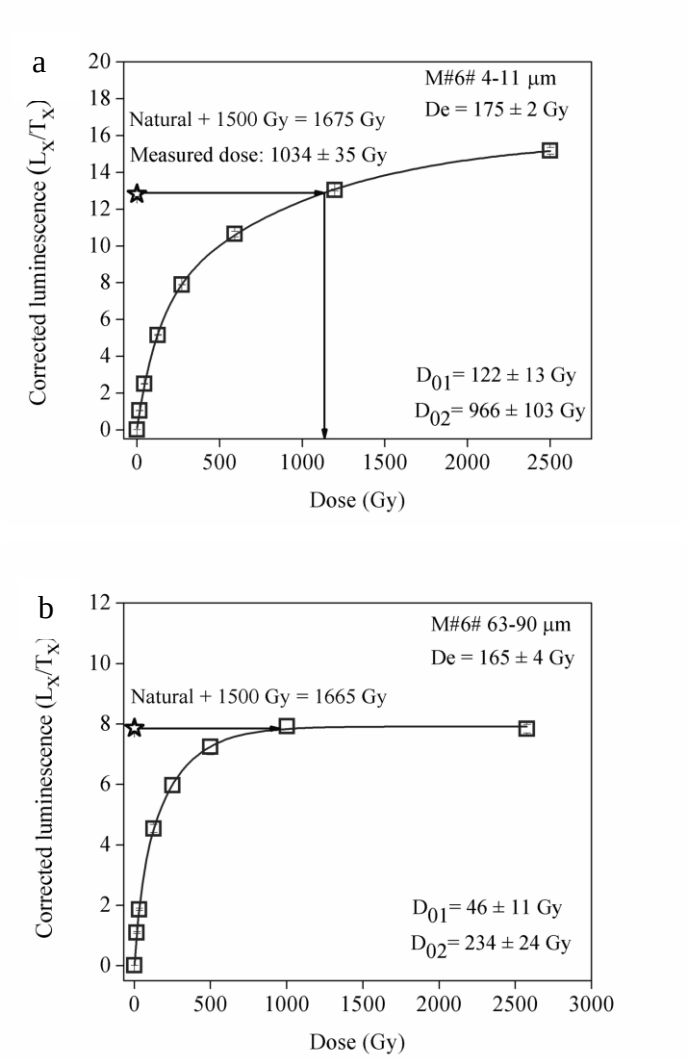

Fig.3.4. Average (n=3) SAR dose-response curves constructed after giving 1500 Gy in addition to the natural dose. (a) Data for 4-11 μm grains from sample M#6#. (b) Same data for 63-90 μm grains from sample M#6#. The sensitivity corrected signal related to the natural plus 1500 Gy dose is shown as a horizontal line projected onto the dose response curve.

In addition, doses of 50, 100, 200, 300, 400, 500, 1000, 1800, 2500, 3825 and 5825 Gy were given to fresh aliquots of 4-11 μm quartz from sample M#6#. A dose response curve was constructed using the resulting values of L_n^*/T_n^* where n indicates the values measured for natural plus added laboratory dose for each dose (**Fig. 3.5a**, squares).

The experiment was repeated on aliquots of 63-90 μm quartz from sample M#11# (D_e = 107 ± 4 Gy). Doses of 50, 200, 500 and 1000 Gy were given in addition to natural aliquots. The resulting values of L_n^*/T_n^* are plotted in **Fig. 3.5b** (squares) as function of the total dose (Natural+added dose). The doses given in addition to the natural were selected so that the total dose matched the doses used to construct corresponding SAR dose response curves (measured using a tipycal SAR sequence) (**Fig. 3.5a** and **b** for fine and coarse quartz, circles).

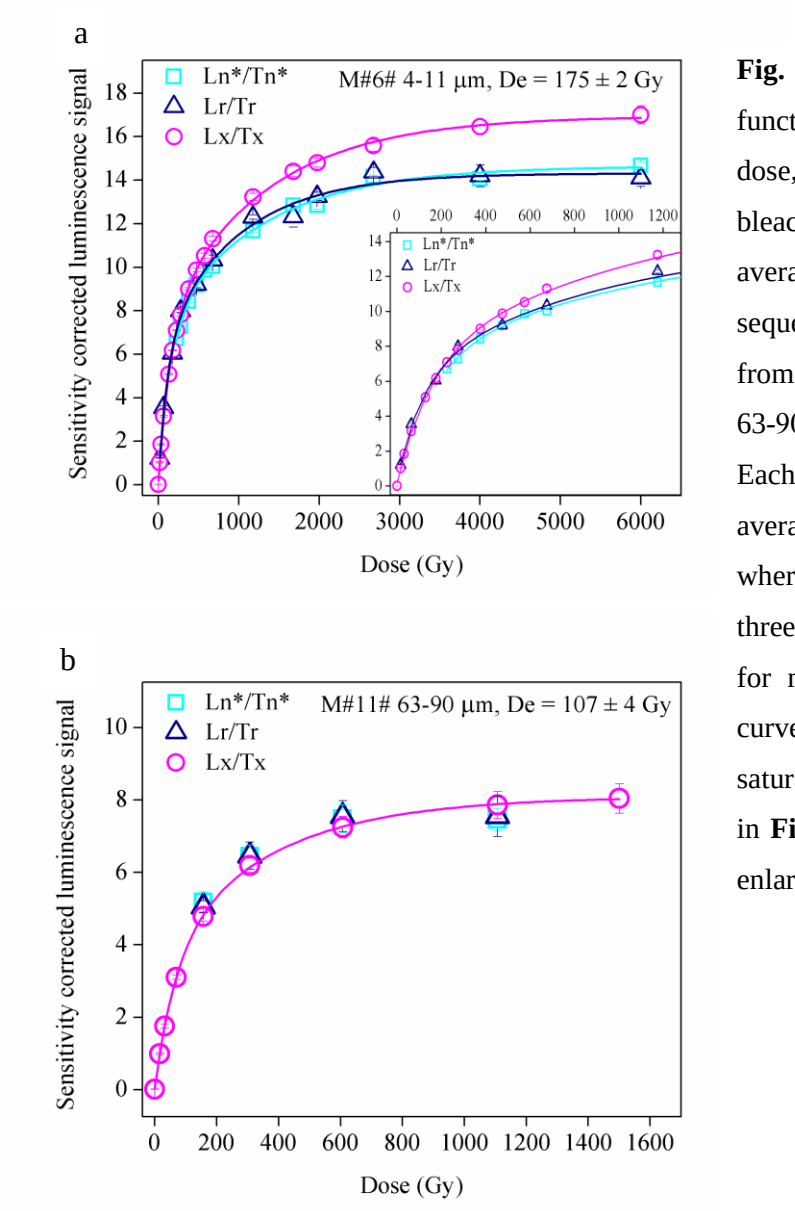

Fig. 3.5. Average L_n*/T_n* plotted as a function of equivalent dose + laboratory dose, average L_r/T_r measured after one bleach as in dose recovery test and average L_x/T_x measured in a SAR sequence. (a) Data for 4-11 µm quartz from sample M#6#. (b) Same data for 63-90 µm quartz from sample M#11#. Each measurement on fine quartz is the average of three to thirteen aliquots, whereas for the coarse fraction between three and seven aliquots have been used for measurements. The dose response curves were fitted using the sum of two saturating exponential functions. Inset in **Fig 3.5.a** presents the same data but enlarged for the low dose region.

A third dose response curve was obtained using measurements made when doses of value equivalent to the natural plus added dose were given after light exposures similar to those applied in a dose recovery experiment, namely two 100 s blue light exposures at room temperature, separated by a 10 ks pause (Murray and Wintle, 2003). The dose response curve derived for the fine fraction from L_r/T_r, where L_r is the response to the dose after this treatment, is also shown in **Fig 3.5a** (triangles). This data set overlaps the dose response curve obtained when doses are added to the natural (L_n*/T_n*), but both of them deviate from the SAR dose response curve for doses of over ~300 Gy. The data sets were fitted with two saturating exponential components. For the 63-90 µm fraction of sample M#11#, the L_r/T_r data set is given in **Fig 3.5b** (triangles). The values of both L_r/T_r and L_n/T_n overlap the SAR dose response curve. Again, the extended SAR dose response curve was best represented by the sum of two saturating exponential functions. For the fine quartz fraction,

both data sets show a greater underestimation compared to the SAR dose response curve when larger doses are given.

3.3.4.1.1. Dose recovery tests

For those aliquots of fine and coarse quartz given laboratory doses in addition to their natural dose, growth curves were constructed using the SAR protocol and the values of D_e obtained for the natural plus added doses were derived. The measured values for the fine fraction for total doses of 225, 275 and 375 Gy are underestimated by 9%, but the underestimation increases to 50% for 2500 Gy. With regard to the coarse quartz, the value measured for 50 Gy added to the natural dose (equivalent to a natural dose of 157 Gy) is underestimated by 6%, but the underestimation increases to 60% for 1000 Gy.

All doses given within the dose recovery test for the coarse quartz from sample M#11# were measured as unknown by the SAR protocol. As expected, the values for the recovered doses are very similar to those obtained for the same sample when doses are added to the natural. This data is not available for the fine quartz fraction of sample M#6#.

3.3.4.2. Quartz from loess

To test whether this dose dependent deviation of the SAR dose response curve from that obtained when doses are added to the natural is a more general effect, measurements similar to those performed in **Section 3.3.4.1** for quartz from aeolianites were also carried out for fine (4-11 μm) and coarse (63-90 μm) quartz from sample XF 153 from Xifeng loess-paleosol section in China (Timar-Gabor et al., 2017). A comparison between the L_n*/T_n*, L_r/T_r and L_x/T_x values is given in **Fig. 3.6a** and **b** for fine and coarse separates, respectively. As was also found for quartz extracted from aeolianites (**Fig. 3.5**), the L_n*/T_n* values obtained for natural plus added doses on fine quartz from loess match the L_r/T_r values obtained when doses are given after removing the natural signal, but both data sets deviate from the L_x/T_x values induced by equal size regenerative doses. This deviation occurs at doses higher than 500 Gy and the degree of underestimation of L_n*/T_n* and L_r/T_r values compared to the L_x/T_x values increases with the given irradiation dose. The data sets were fitted with the sum of two saturating exponential functions. Regarding the coarse material, no significant deviation occurs between the data sets.

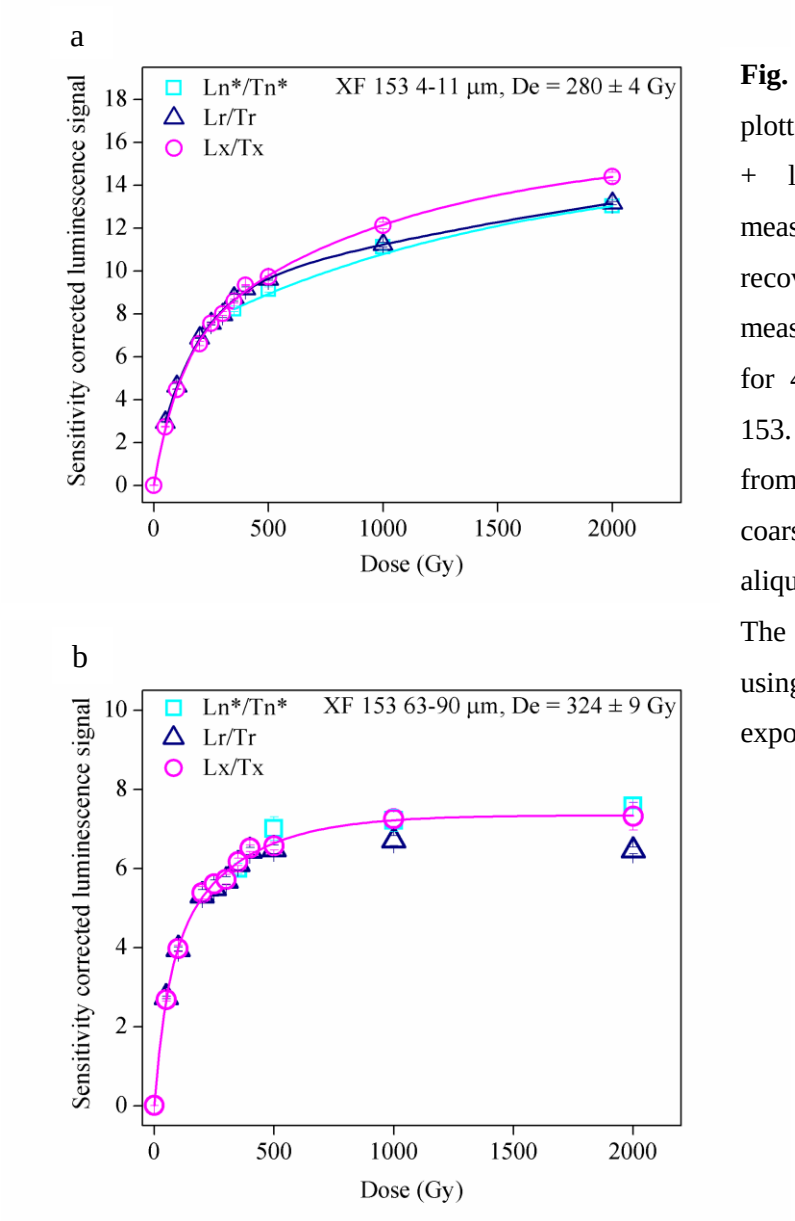

Fig. 3.6. Average L_n^*/T_n^* values plotted as a function of equivalent dose + laboratory dose, average L_r/T_r measured after one bleach as in dose recovery and average L_x/T_x values measured in a SAR sequence. (a) Data for 4-11 µm quartz from sample XF 153. (b) Same data for 63-90 µm quartz from sample XF 153. For both fine and coarse quartz, between two and four aliquots were used for measurements. The dose response curves were fitted using the sum of two saturating exponential functions;

3.3.4.2.1. Dose recovery tests

The D_e values measured for the Chinese loess sample (XF 153) when doses are added to the natural dose for both fine and coarse quartz show an underestimation of ~10% even for added doses as low as 70 Gy for fine and 26 Gy for coarse quartz (equivalent to natural doses of 350 Gy). The values measured for fine and coarse quartz from the same sample when doses are given within the dose recovery test are not underestimated by more than 10% for doses up to 500 Gy.

3.4. Discussion

Using the SAR protocol, the 4-11 µm and coarse (63-90, 90-125, 125-180, 180-250 µm) grains from the aeolianites gave ages which were in agreement, allowing average ages to be calculated as given in **Table 3.1**.

The SAR dose response curves obtained for the 4-11 μm grains and the coarse grained quartz are best represented by the sum of two saturating exponential functions and are quite different (**Fig. 3.1**), as was also found for the quartz extracted from Romanian, Serbian and Chinese loess (Timar-Gabor et al. 2015a; Timar-Gabor et al., 2017).

The normalised light levels (L_n*/T_n*) for a 63–90 μm aeolianite quartz sample, obtained when doses are added to the natural dose overlap the L_x/T_x values measured in a typical SAR dose response curve (**Fig. 3.5b**). A similar result was obtained for 63–90 μm quartz from loess (XF 153) from China (**Fig. 3.6b**). Moreover, for aeolianite quartz, when doses are given after a double exposure to blue light, as in the standard dose recovery test (Murray and Wintle, 2003), the dose response (L_r/T_r) also matches the SAR curve (L_x/T_x), while for the loess quartz sample the L_r/T_r are slightly underestimated when compared to the L_x/T_x data set. This may suggest that the dose response curves for the coarse grains, even though constructed using two saturating exponential components, can be regarded as more reliable for D_e evaluation than for the fine grains.

Values of L_n*/T_n* obtained for quartz from both aeolianite and loess when a dose is added to the natural dose for 4–11 μm grains result in a dose response curve that does not reach the same level of saturation as the SAR response curve L_x/T_x (see **Fig. 3.5a** and **Fig. 3.6a**). For the aeolianite quartz, this underestimation is less than 8% for doses up to ~600 Gy, but increases to 15% in a way which is dose dependent (**Fig. 3.6a**). When quartz from loess is used, the underestimation of the L_n*/T_n* values relative to the L_x/T_x values increases from 4% for 350 Gy to 10% for 2000 Gy. When samples are given a double exposure to blue light, the dose response L_r/T_r for 4–11 μm quartz grains from aeolianites and loess also deviates from the SAR curve given by L_x/T_x (see **Fig. 3.5a** and **Fig. 3.6a**). For doses up to ~1200 Gy the underestimation is less than 10%, but increases to 17% for 6000 Gy in the case of quartz from the aeolianite sample (**Fig. 3.5a**). Using quartz from loess, this underestimation does not exceed 10% even for doses as high as 2000 Gy, but the degree of underestimation increases with the given irradiation dose (**Fig. 3.6a)**.

Our approach of adding doses in addition to the natural dose is similar to the philosophy of the Australian slide method used for thermoluminescence (TL) dating (Prescott et al., 1993). It is interesting to note that a similar inability to overlay dose response curves was observed in TL studies using the blue emission of coarse quartz (e.g. 90-125, 180-250 μm) (Prescott et al., 1993). In the case of those emissions, an anomalous radiation response of quartz at radiation doses above 300 Gy has been reported (Huntley and Prescott, 2001) based on the observation of a mismatch between the natural plus added dose and the regenerated dose curves. The cause of these observations is yet unknown.

3.5. Conclusions

The results for the aeolianites from the western Mediterranean confirm that the discrepancies between dose response curves for these two grain sizes in Romanian, Serbian and Chinese loess are part of a widespread phenomenon. For doses up to about ~200 Gy, the laboratory dose response curves for the two grain sizes from the aeolianite are able to be superimposed. In addition, the ages obtained for doses up to 170 Gy using different grain sizes are in agreement. The concordance of the ages implies that the SAR protocol can be applied to either grain size back to about ~250 ka for the aeolianites in the current study.

Based on the dose dependent deviation of the SAR dose response curve from those obtained when doses are added to the natural as well as when they are added after removing the natural signal, 4-11 μm quartz grains should not be used for expected values of D_e in the high dose range; a clearly defined high dose range cannot be given based on this data, but determining doses of a few hundred Gy using fine quartz and the SAR protocol should be regarded with caution. This dose dependent deviation is much less pronounced for coarse grains and it seems reasonable to infer that the dose response curves for the coarse grains, although saturating earlier, can be regarded as more reliable for equivalent dose calculation than those for the fine grains. However, these observations raise doubts about the accuracy of the SAR protocol when applied in the high dose range, in particular in the case of the fine quartz fraction.

4 Single and multi-grain OSL investigations in the high dose range using coarse quartz – based on Anechitei-Deacu et al. (2018b)

4.1. Introduction

Various studies carried out over the past decade using quartz from samples with independent age control (e.g. Murray et al., 2007; Buylaert et al., 2008; Lai, 2010; Timar-Gabor et al., 2011; Constantin et al., 2014) produced evidence of systematic equivalent dose underestimation when the paleodoses are higher than 100-200 Gy. Moreover, it was found that the natural OSL signal of 'infinitely' old samples from Romanian (Timar-Gabor et al., 2012) and Chinese loess (Buylaert et al., 2007) was not in laboratory saturation.

The present work aims at obtaining more insights into these observations by investigating the degree of correspondence between the natural OSL signal and the SAR laboratory saturation level for an 'infinitely'old sample collected below the Brunhes/Matuyama boundary at Roksolany loess profile (Ukraine). Extended dose response curves are constructed for coarse (180-250 μm) quartz from this sample using both single-grain and multi-grain aliquot approaches. We also compare the luminescence properties of the 180-250 μm quartz extracted from sample ROX 1.14 with those of 90-125 μm quartz extracted from the same sample.

4.2. Experimental details

4.2.1. Samples

The sample used in this study was collected from the Roksolany loess-paleosol section on the northern Black Sea coast of the Ukraine. It was taken from the base of the profile (~45 m depth) below the Brunhes/Matuyama (B/M) polarity transition that was previously identified based on paleomagnetism measurements (Tsatskin et al., 1998; Dodonov et al., 2006). Since the investigated sample (coded ROX 1.14) was collected from loess approximately 10 m below the ~780 ka ago Brunhes/Matuyama polarity transition, an age of ≥800 ka is expected for this sample. Given the measured dose rate of 2.1 ± 0.1 Gy/ka, ROX 1.14 is expected to have a minimum paleodose of ~1700 Gy. Electron spin resonance (ESR) dating using Al-hole center signals and Ti signals gave equivalent doses of >2000 Gy (see **Section 4.3**), consistent with expectations.

4.2.2. Instrumentation and measurement protocols

Multi-grain luminescence measurements were carried out using TL/ OSL Risø DA-20 readers (Bøtter-Jensen et al., 2010). A single grain laser attachment (Bøtter-Jensen et al., 2003) was used for single-grain luminescence measurements of quartz. The stimulation source is a

10mWNd:YVO_4 solid-state diode pumped laser emitting at 532 nm, which can be focused sequentially onto a square grid of 100 grain holes in an aluminium sample disc.

For both single and multi-grain aliquot extended dose response curves, a double SAR protocol (Roberts and Wintle, 2001) employing an IR stimulation at 125 ºC (for 40 s) prior to blue or green stimulations was used. Green laser stimulation at 125 ºC was performed for 0.9 s in the case of single-grain measurements. Blue or green LED stimulations for 40 s at 125 ºC were used for stimulating multi-grain aliquots. In the case of the single-grain analyses, the signal was summed over the initial 0.06 s of stimulation, whereas the background was evaluated from the final 0.15 s, i.e. late background subtraction. For the multi-grain-analyses, the signal was summed over the first 0.308 s of the decay curve and the background was assessed from the 1.69-2.30 s interval, i.e. early background subtraction.

Electron spin resonance analyses were carried out using a Bruker EMX + spectrometer. Samples were measured in the X band at 90 K using a variable temperature unit. A high sensitivity cavity was used and samples were rotated in the cavity for collecting several spectra using a programmable goniometer. Signals were quantified using peak to peak height from g=2.018 to g=1.993 in the case of Al signals as recommended by Toyoda and Falguères (2003), and from g=1.978 to g=1.913 in the case of Ti respectively, 'option A' in Duval and Guilarte (2015). Irradiations were performed using a Nordion Gammacell 220 Co-60 gamma irradiator.

4.3. Experimental results and discussions

4.3.1. Electron spin resonance equivalent doses

We have derived equivalent doses using both Al and Ti signals for 125-180 µm quartz from ROX 1.14. Recently, Duval et al. (2017) recommend that such a multiple center approach should become part of the standard dating procedure. In order to test the procedure, but also to obtain data needed for further bleaching corrections for sample ROX 1.14, we have applied the method to a modern analogue, a Holocene sample with a known age obtained by quartz OSL dating. The equivalent dose (~14 Gy) of this modern analogue is thus negligible compared to the natural dose (>1700 Gy) received by sample ROX 1.14. The ESR signals measured for this modern analogue were used for correcting the ESR signals recorded for sample ROX 1.14, measured in a standard multiple aliquot approach (**Fig. 4.1**). The corrected equivalent doses for sample ROX 1.14 using 125-180 µm quartz are 2100 ± 300 Gy for Al-hole signals and 2830 ± 50 Gy for Ti signals. Although the agreement is probably not within uncertainty, derived ages of 1000 ± 160 ka for Al signals and 1360 ± 90 ka for Ti signal confirm an age older than the timing of the Brunhes/Matuyama transition for sample ROX 1.14 and gives us confidence that the sample can be considered as 'infinitely' old from the perspective of quartz OSL dating.

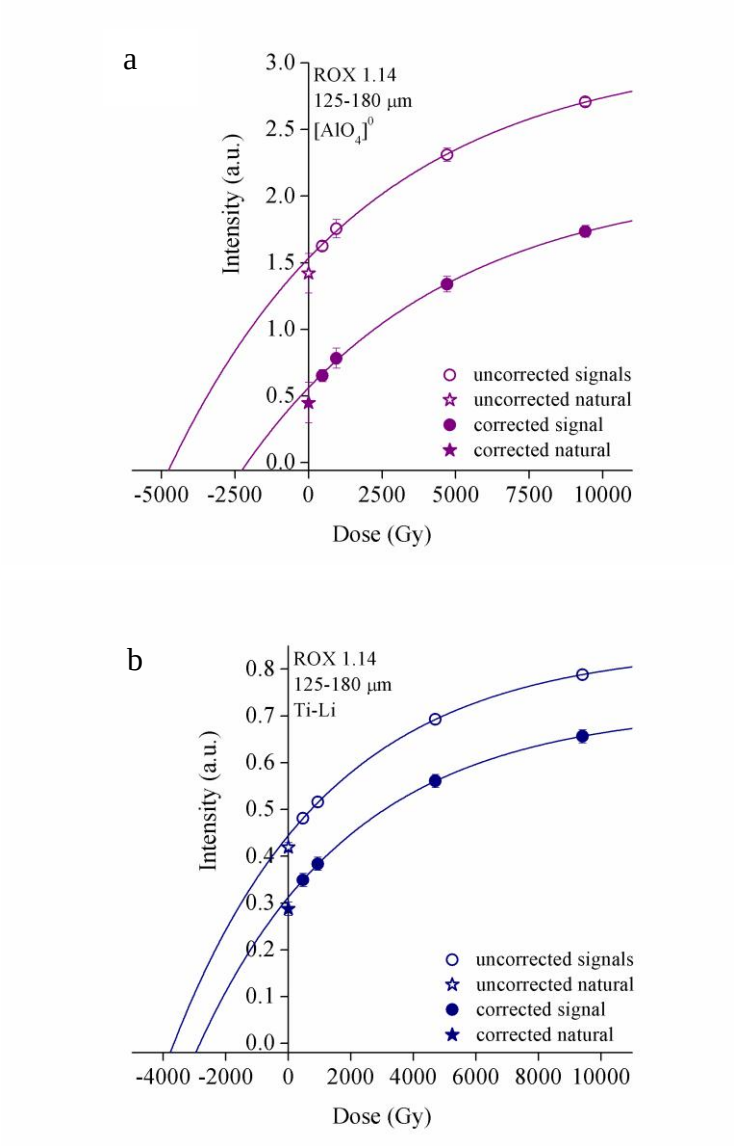

Fig. 4.1. Dose response curves for Al (a) and Ti (b) paramagnetic centres for ROX 1.14 125-180 µm quartz. In the case of Al signals each data point represents the average peak to peak intensity derived from 4 measurements, while in the case of Ti-signals measurements were carried out twice. Open symbols represent the signals measured following gamma dose irradiation on top of the natural accrued dose, while filled symbols represent the values obtained after the correction using the natural signals of the modern analogue sample. Dose response curves were fitted with single saturating exponential functions, with saturation parameters of D_0= 6770 ± 1200 Gy for Al signals and D_0= 4920 ± 90 Gy for Ti signals.

4.3.2. Single aliquot and single grain OSL dose response curves

4.3.2.1. Single aliquot dose response curves

Dose response curves (DRCs) were constructed up to 2500 Gy using 6 multi- and 38 single-grain aliquots (100 grains per single-grain aliquot) of quartz. The average dose response curve of the six multi-grain aliquots is presented in **Fig. 4.2**. The sensitivity corrected (L_x/T_x) laboratory OSL signal is fully saturated by ~1000 Gy, but the natural L_n/T_n only reaches ~86% of the laboratory saturation level. The closeness to saturation of the natural signal was assessed using the $(L_n/T_n)/(L_x/T_x)_{max}$ ratio, where $(L_x/T_x)_{max}$ represents the average value of the data points in the plateau region of the dose response curve. The laboratory dose response for multi-grain aliquots is well represented by the sum of two saturating exponential functions, i.e. $I(D) = I_0 + A*(1 - \exp(-D/D_{01})) + B*(1 - \exp(-D/D_{02}))$, where *I* is the OSL intensity at dose D, I_0 is a residual luminescence signal, *A* and *B* represent the amplitude of the two exponential components and D_{01} and D_{02} are the

doses that characterise the curvature of the DRC. Since the natural signal was not found to be in saturation, finite equivalent doses could be derived for multi-grain aliquots of quartz.

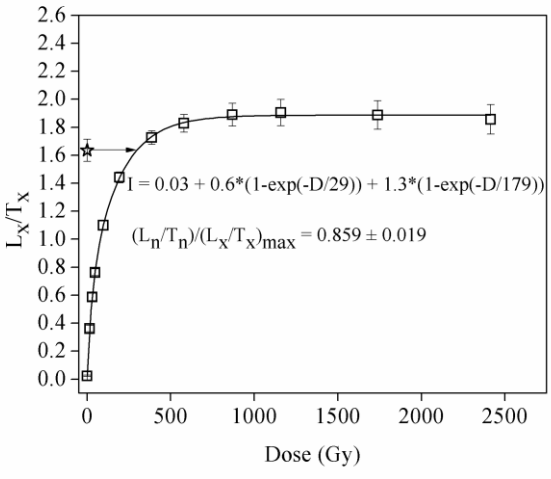

Fig. 4.2. Average (n=6) SAR dose response curve constructed using multi-grain aliquots of quartz. The sum of two saturating exponential functions was used for data fitting.

4.3.2.2. Single grain dose response curves

In the single grain data set, less than 10% of the grains were sufficiently bright (i.e. the response to the test dose was known to better than 20%) to allow a dose response curve to be constructed. The dose response curves are highly variable both in shape and in the position of the natural signal relative to the laboratory saturation level. The single grain data sets are well represented by a single saturating exponential function of the form $I(D) = A *(1 – \exp((-D – xc)/D_0))$, where xc is a dose offset. The characteristic doses (D_0 values) vary over approximately two orders of magnitude.

4.3.2.3. Optical dating

4.3.2.3.1. Annual dose determination

The dose rates were calculated using the concentrations of ^{238}U, ^{232}Th and ^{40}K derived by high-resolution gamma spectrometry and the conversion factors published by Adamiec and Aitken (1998).

4.3.2.3.2. Equivalent doses and OSL ages

The SAR protocol was used to derive equivalent doses. In the case of the multi-grain aliquots, only those aliquots having recycling and IR depletion ratios within 10% from unity and a recuperation value below 5% of the natural were accepted for D_e and age calculation.

For the single-grain data set, a number of 3,800 grains has been measured for ROX 1.14 (180-250 µm). Equivalent doses were determined only for the grains which passed the selection criteria used by Thomsen et al. (2016) i.e., less than 20% relative uncertainty on the natural test dose signal, recycling and IR depletion ratios consistent with unity within two standard deviations, and recuperation values less than 5% of the natural. A number of 184 grains passed the selection criteria described above and the D_e values are shown as frequency histogram in **Fig. 4.3**.

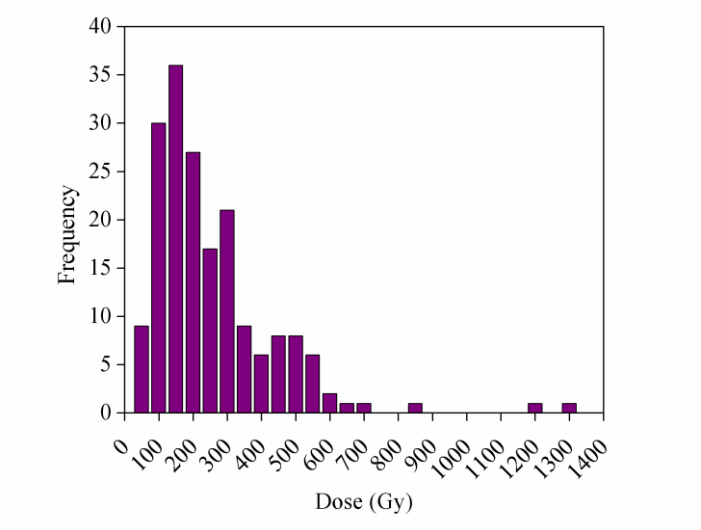

Fig. 4.3. Frequency histogram of the D_e values obtained for individual grains from sample ROX 1.14 (180-250 µm) that passed the selection criteria.

4.3.2.4. Signal intensity variability at individual grain level

Inter-grain OSL intensities for ROX 1.14 are highly variable, the magnitude of the net natural signal ranging from tens of counts to hundred thousand counts recorded in the first 0.06 s of stimulation. The majority of the total OSL signal originates from less than 10% of the measured grains, which is consistent with previously published results for single grains of quartz from sedimentary samples (see **Table 4.1**; see for example Duller, 2006).

The grains with natural OSL signals of more than 50 counts recorded in the first 0.06 s of stimulation (353 out of 3,800 measured grains) were classified into five groups based on the intensity of their net natural signal or natural test dose response. The absolute and relative contributions from each group of grains to the total light sum (of the 3,800 measured grains) for both natural and first test dose signal and the number of grains in each group are given in **Table 4.1**. More than 70% of the natural and first test dose signals originate from most bright 44 grains which make up ~1.2% of the total measured grains.

Table 4.1. Classification of the individual grains into five groups based on the intensity of their net natural signal (counts collected in the first 0.06 s of stimulation). The absolute and relative contributions of each group to the total light sum are given. Note that no grains were found in 9,000 to 18,000 counts group.

-	Sum of all grains	Sum of grains with between:					
-	-	130,000-18,000 counts (Super bright grains)	9,000-2,000 counts	2,000-500 counts	500-200 counts	200-50 counts	130,000-50 counts
Number of grains	3,800	4	40	59	73	177	353
L_n net (counts)	523,408	252,736	166,851	51,056	23,207	17,995	511,844
T_n net (counts)	331,871	136,403	108,803	38,964	15,676	14,710	314,556
% of the total signal for L_n	100%	48.3%	31.9%	9.8%	4.4%	3.5%	98%
% of the total signal for T_n	100%	41.1%	32.8%	11.7%	4.7%	4.5%	95%

4.3.3. Multi and single-grain synthetic dose response curve

A multi-grain synthetic aliquot dose response curve was constructed using the summed OSL signals (summed L_x divided by summed T_x) from the six measured multi-grain dose response curves. The resulting OSL signal and dose response curve are equivalent to that of one large single aliquot containing all the grains from six multi-grain discs. The synthetic dose response curve is displayed in **Fig. 4.4a** and it can be seen that the natural signal is at 86% of the laboratory saturation level.

Using single-grain data the individual OSL signals from each measured grain (3,800 in total) were summed, in the attempt to reproduce the single aliquot measurement results. A single-grain aliquot synthetic DRC was constructed using the summed OSL signals from the 3,800 individual grains. The L_n/T_n value of this single-grain synthetic DRC is 92% of the laboratory saturation level (**Fig. 4.4b**).

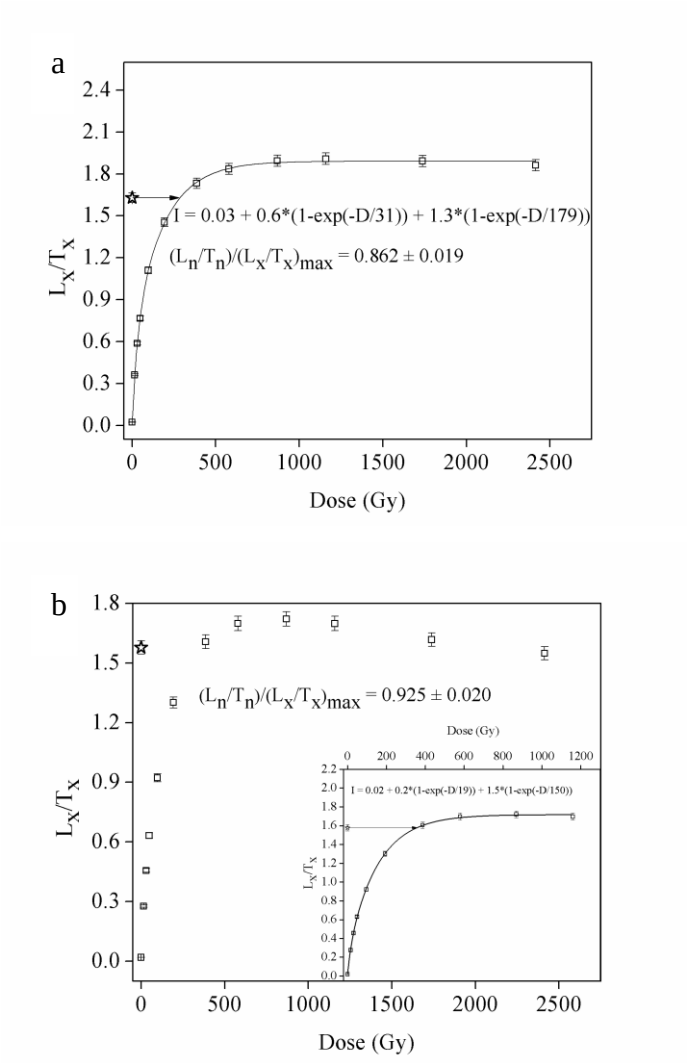

Fig. 4.4. Synthetic dose response curve constructed using (a) the summed OSL signals from 6 multi-grain aliquots and (b) the summed OSL signals from 3,800 individual grains of quartz. Data are fitted using a sum of two single-saturating exponential functions. In order to obtain a reliable fitting of the dose response curve in (b), the last two L_x/T_x point were removed.

4.3.4. Blue versus green light stimulation

One possible explanation for the difference observed between the fraction of laboratory saturation of the natural signal in the case of multi and single-grain synthetic aliquots may be that optical stimulation was carried out at different wavelengths, i.e. 470 nm (blue) and 532 nm (green) for multi and single-grain measurements, respectively. Singarayer and Bailey (2004) have shown that the bleaching rate of the fast and medium components is wavelength dependent.

To test whether green light stimulation gives rise to a higher $(L_n/T_n)/(L_x/T_x)_{max}$ ratio than the ratio obtained using blue light stimulation, three multi-grain dose response curves were constructed using green light (532 nm, 40 mW/cm^2) stimulation. Again, the natural signal is only 83% of the laboratory saturation. This value is consistent with that obtained when the luminescence signal from multi-grain aliquots was stimulated with blue light. Therefore it is concluded that stimulation with different wavelengths is not the cause of overestimation of the natural L_n/T_n saturated signal by the laboratory DRC in the case of the single-grain synthetic DRCs compared to the multi-grain synthetic DRCs.

4.3.5. Natural signal saturation level as function of brightness

4.3.5.1. Single grain data

4.3.5.1.1. Sample ROX 1.14 180-250 μm

Since the luminescence signal from a multi-grain aliquot is the sum of the signals from all individual grains making up the aliquot, the difference in the closeness of the natural signal to saturation when comparing single-grain to multi-grain synthetic aliquot DRCs may be the result of a different relative contribution from populations of grains with different characteristics.Variability in the luminescence brightness of individual grains from a sample plays a major role when a number of individual signals are added as the very bright grains dominate the total light sum.

In order to evaluate the importance of such differential contributions, for each group of grains (as described in **Section 3.2.1**) single-grain synthetic DRCs were constructed by summing the signals from the individual grains. The corresponding sensitivity corrected natural signal was then interpolated onto these synthetic DRCs. The sensitivity corrected natural light level is closer to the laboratory saturation level as the brightness of the grains increases.

By plotting the $(L_n/T_n)/(L_x/T_x)_{max}$ ratios as function of the average number of counts collected in the first 0.06 s of stimulation for the natural signal of the grains in each group (**Fig. 4.5**, red circles) it can be observed that the ratio increases from 0.81 for the group containing grains with a natural net OSL between 50-200 cts collected in the first 0.06 s of stimulation, to 0.98 for the super bright grains group (>18,000 counts recorded in the first 0.06 s of stimulation). Since the natural signals are expected to show a higher degree of inherent variability due to e.g. microdosimetric effects, the grains were also sorted according to the intensity of the first test dose signal (T_n) which should not be influenced by such issues; the resulting $(L_n/T_n)/(L_x/T_x)_{max}$ ratios for each group of grains are plotted against the average number of counts collected in the first 0.06 s of stimulation in **Fig 4.5** (black circles). The two data sets are very similar, indicating that signal selection has no significant impact on the observed trend.

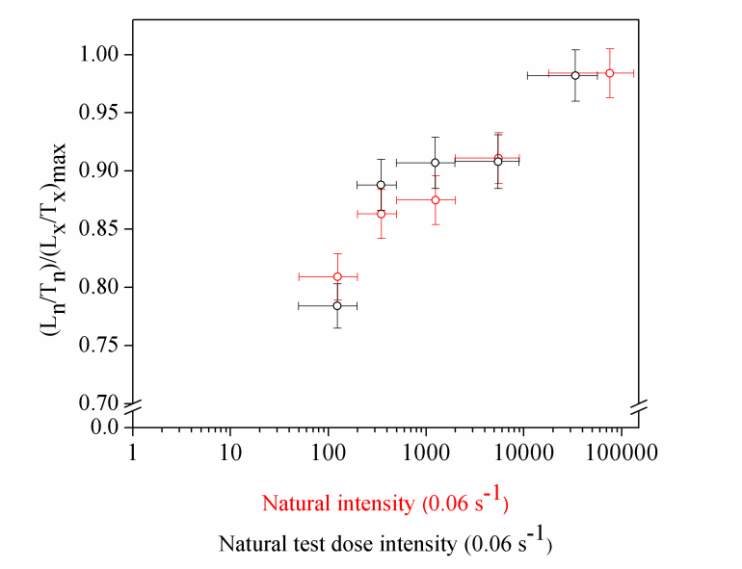

Fig. 4.5. The ratios $(L_n/T_n)/(L_x/T_x)_{max}$ for ROX 1.14 180-250 μm as function of the average number of counts recorded in the first 0.06 s for the natural signal of the grains in each group are shown as red circles. Same data obtained for groups of grains constituted based on the intensity of the first test dose signal are represented with black circles.

4.3.5.1.2. Sample ROX 1.14 90-125 μm

A data set similar to that presented in **Section 4.3.5.1.1** was obtained for the 90-125 μm quartz fraction extracted from sample ROX 1.14. Dose response curves were constructed up to 2500 Gy for 15 single-grain aliquots (totalising 1,500 grains). A number of 93 grains were identified to have natural OSL signals of more than 50 counts recorded in the first 0.06 s of stimulation. They were further classified into three groups based on the intensity of their net natural signal. The grains were also grouped according to the intensity of the first test dose signal. Again, the $(L_n/T_n)/(L_x/T_x)_{max}$ ratio increases as function of the signal brightness (**Fig. 4.6**). The increase is less pronounced than that observed for the 180-250 μm quartz fraction, but this is not surprising considering the lower number of grains measured for the 90-125 μm fraction and the lack of super bright grains.

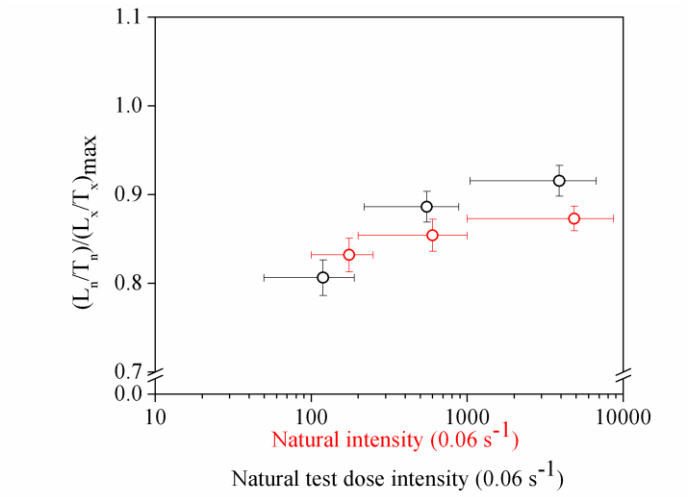

Fig. 4.6. The ratios $(L_n/T_n)/(L_x/T_x)_{max}$ for ROX 1.14 90-125 μm as function of the average number of counts recorded in the first 0.06 s for the natural signal of the grains in each group are given as red circles. Same data obtained for groups of grains formed based on the intensity of the first test dose signal are shown as black circles.

4.3.5.2. Implications for multi-grain aliquots.

We now investigate whether the correlation between the closeness to saturation of the natural signal and the brightness of individual grains is reflected in the multi-grain data. Investigations on multi-grain aliquots of quartz from ROX 1.14 were not possible due to insufficient coarse material. To explore the existence of such a dependency in multi-grain aliquots, data for the oldest four samples collected from L2 unit (corresponding to MIS 6) at the Costinesti loess-paleosol section in Romania were re-analysed (for the 63-90 μm quartz fraction). This section was previously described by Timar-Gabor and Wintle (2013) and Constantin et al. (2014) and samples CST 22 – CST 25 were previously shown to be in field saturation. $(L_n/T_n)/(L_x/T_x)_{max}$ ratios were calculated for these samples. The considered value for $(L_x/T_x)_{max}$ is the value obtained for a regenerative dose of 1000 Gy which is a high enough dose for the laboratory signal to be in saturation (see Timar-Gabor et al., 2017). Increasing $(L_n/T_n)/(L_x/T_x)_{max}$ ratio can be observed as function of the signal brightness for both natural (**Fig. 4.7a, b, c, d**) and first test dose (Fig. **4.7e, f, g, h**) signals.This indicates that the dependency of the $(L_n/T_n)/(L_x/T_x)_{max}$ ratio on the brightness of the grains observed for the single-grain synthetic aliquots is also detectable at the multi-grain aliquot level.

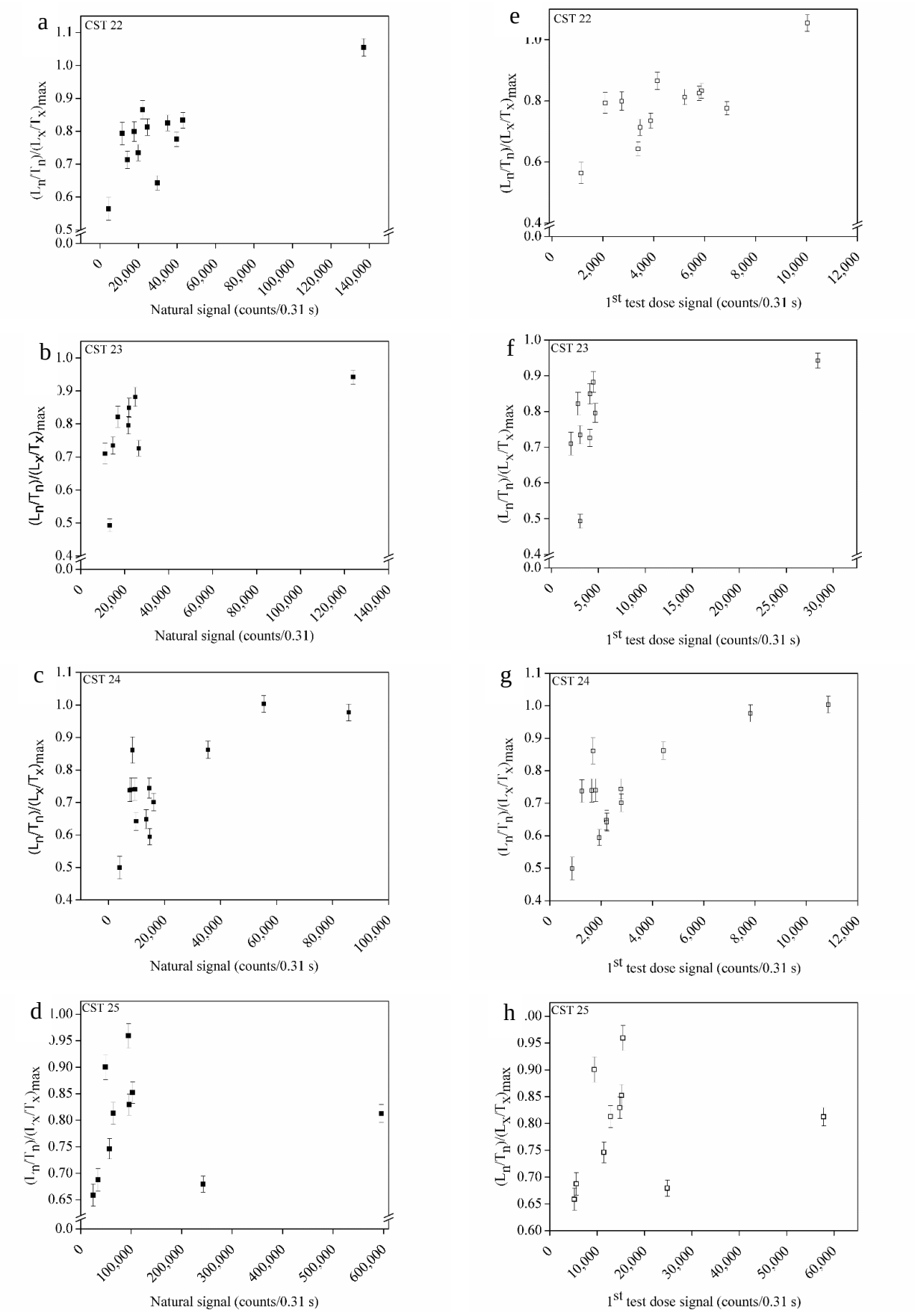

Fig. 4.7. The $(L_n/T_n)/(L_x/T_x)_{max}$ ratios for 63-90 μm quartz samples from Costinesti loess profile, as function of the number of counts collected in the first 0.31 s for (a), (b), (c), (d) the natural signal and (e), (f), (g), (h) the first test dose signal.

4.4. Conclusions

Single and multi-grain single aliquot regenerative (SAR) OSL investigations were carried out for a coarse-grained (180-250 μm) quartz sample extracted from loess collected below the Brunhes/Matuyama transition at the Roksolany section in Ukraine. The aim was to investigate the consistency of the sensitivity-corrected natural OSL signal and the laboratory SAR saturation level. Electron spin resonance dating of this sample using a multiple center approach (Al and Ti signals) resulted in ages above 1000 ka, confirming that the accrued dose (about 2000 Gy) of the sample falls beyond the limit of standard OSL equivalent dose measurement techniques.

It was found that for the single-grain synthetic DRC the natural signal is closer to the laboratory saturation level (92%) than in the case of the multi-grain synthetic DRC (86%). This difference can not be attributed to different stimulation wavelengths, i.e. blue and green light stimulation for multi- and single-grain measurements, respectively.

When groups of grains were synthetically formed based on the intensity of either the natural signal or the first test dose signal, it was observed that the $(L_n/T_n)/(L_x/T_x)_{max}$ ratio increases as function of the signal brightness. This pattern is confirmed for 90-125 μm quartz grains extracted from the same sample (ROX 1.14). Although less clear, a similar trend was observed for multi-grain aliquot data obtained for coarse-grained (63-90 μm) quartz extracts from Costinesti (Romania) loess-paleosol section. It is concluded that variations in the contribution from populations of grains with different levels of brightness can be considered a controlling factor in the closeness of the natural signal to laboratory saturation SAR OSL level for this ‘infinitely’ old sample.

The results obtained in this study contribute to a better understanding of previously reported cases in which the natural signal of ‘infinitely old’ quartz samples was found to be below the laboratory saturation level. Further OSL investigations are needed in order to examine whether this finding contributes to the underestimation often reported in literature for quartz samples with expected paleodosesdoses higher than ~200 Gy.

Conclusions

Optically stimulated luminescence (OSL) dating of quartz was revolutionised by the development of the single-aliquot regenerative-dose (SAR) protocol and it is currently one of the most valuable chronological tools available for Quaternary studies. The real potential of SAR-OSL dating of quartz is hindered by a range of problems; one of the most important is the age underestimation increasingly reported in the past years and which in most of the cases is unrelated to closeness of the natural OSL signal to the level of the laboratory saturation. SAR-OSL age

underestimation beyond 40 ka (D_es usually >100-200 Gy) was reported for either fine (4-11 μm) or coarse (different fractions in the range 63-250 μm) quartz samples from different geological contexts around the world, despite the good agreement of the ages for the younger samples with independent age control.

When SAR-OSL investigations were performed on fine (4-11 μm) and coarse (63-90 μm) quartz extracted from Romanian, Serbian and Chinese loess, additional issues were reported. The dose response curves (DRCs) constructed using fine and coarse quartz fractions were found to have different growth patterns, with the signal of the fine grains showing much higher saturation characteristics. The sensitivity corrected OSL signal is in full saturation for the coarse fraction at doses higher than ~ 500 Gy while the fine fraction dose response curve reaches its plateau only in the dose recgion above ~2000 Gy. DRCs of both grain fractions are being well represented by a sum of two saturating exponentials (see for example Timar-Gabor et al., 2012; Constantin et al., 2014; Timar-Gabor et al., 2015b). Another important observation regards the inconsistency of the natural- and laboratory-induced DRCs for both fine and coarse quartz (Timar-Gabor and Wintle, 2013; Timar-Gabor et al., 2015b). It was found that the natural dose response curve can befitted using one saturating exponential function, whereas a sum of two such functions is required to describe the growth of the laboratory dose response curves. Moreover, the laboratory DRCs continue to grow at doses higher than 300 Gy, whereas the natural DRCs show no growth in this region. In the fine quartz fraction, the difference between the natural and laboratory DRCs is more clear and pronounced compared to coarse quartz.

Both the divergence between fine- and coarse-grained quartz DRCs and between natural and laboratory DRCs start at doses above ~100-200 Gy (Timar-Gabor and Wintle, 2013; Timar-Gabor et al., 2017**)**. It is believed that the equivalent doses (D_es) obtained above this dose range and corresponding OSL ages (>~40 ka) for coarse quartz are higher compared to those for the fine fraction and the underestimation of the D_e values and consequently OSL ages occurs with an earlier and more severe underestimation in the case of fine quartz as a consequence of these inconsistencies (Timar-Gabor et al., 2011; Constantin et al., 2014; Constantin et al., 2015; Timar-Gabor et al., 2015b).

We extended the investigations using fine (4-11 μm) and different coarse quartz (>63 μm) grains extracted from aeolianites from a site on the Eivissa Island (southwestern Mediterranean) (del Valle et al., 2016, Anechitei-Deacu et al., 2018a). Aeolianites were chosen since they contain quartz from a different geological context and have significantly lower environmental dose rates compared to loess. The dose response curves of the OSL signals for fine and coarse quartz are similar to those for quartz from loess, with the OSL response of the fine quartz growing to higher doses than the signal for the coarse fraction; the growth of the signal with dose and is also

represented by the sum of two saturating exponential functions. We provided evidence that the saturation parameters are not meaningful unless high enough doses (> 1 kGy) are given for the OSL to reach saturation. We also compared the luminescence properties of quartz from these aeolianites with those for quartz extracted from a sample of loess from Xifeng, China.

For doses up to ~200 Gy, the dose response curves of fine and coarse grains from aeolianites can be superimposed and the ages obtained for the different grain sizes are in agreement up to ~250 ka, increasing our confidence in the accuracy of the ages obtained for samples with such doses, irrespective of the magnitude of the environmental dose rate. Particularly for the fine quartz fraction, a mismatch between the SAR dose response curve and the dose response curve obtained when doses are added to the natural is reported, indicating that the application of the SAR protocol in the high dose range is problematic. This dose dependent deviation is much less pronounced for coarse grains. Thus, it seems reasonable to infer that the dose response curves for the coarse grains, although saturating earlier can be regarded as more reliable for equivalent dose calculation than those for the fine grains (Anechitei-Deacu et al., 2018a).

Previous observations reported that the natural OSL signal of 'infinitely' old samples from Romanian and Chinese loess was found not tobe in saturation. New insights into this issue were gained by investigating the degree of correspondence between the natural OSL signal and the SAR laboratory saturation level for an 'infinitely' old sample. Single and multi-grain SAR-OSL investigations were undertaken for a coarse-grained (180-250 μm) quartz sample extracted from loess collected below the Brunhes/Matuyama transition at the Roksolany site (Ukraine). The sample was dated to more than 1000 ka by electron spin resonance using a multi center approach (Al and Ti signals), confirming that the D_e (~2000 Gy) falls beyond the limit of standard OSL D_e measurement techniques. However, the natural signal measured using multi-grain aliquots of quartz was found to be below the laboratory saturation level.

A comparison was made between synthetic dose response curves generated from single-grain and multi-grain aliquot data, respectively; the natural signal was found to be closer to the laboratory saturation level (92%) in the case of the single-grain synthetic DRC than for the multi-grain synthetic DRC where the signal was 86% of the saturation level. This difference could not be attributed to stimulation with different wavelengths, i.e. blue and green light stimulation for multi and single-grain measurements, respectively. By analysing synthetic data obtained by grouping grains according to their brightness, it was observed that brighter grains give a natural signal closer to the laboratory saturation level. Similar results were obtained for another quartz fraction (90-125 μm) extracted from the same sample. This trend (brighter aliquots displaying a natural signal closer to the laboratory saturation level) was also confirmed for multi-grain aliquot data. Based on these findings we infer that variability in the contribution from populations of grains with different levels

of brightness may represent a controlling factor in the closeness of the natural signal to laboratory saturation level for infinitely old samples (Anechitei-Deacu et al., 2018b).

A combined approach including OSL, TL, electron spin resonance (ESR) and other physical methods (e.g. spatially resolved luminescence, IR spectroscopy, X-ray difraction) applied comparatively on grains with different levels of brightness has the potential to give key insights into the physical properties differentiating between bright and dim grain and could eventually lead to a better understanding of the processes contributing to the luminescence emission from quartz.

References

Adamiec, G. and Aitken, M., 1998. Dose-rate conversion factors: update. Ancient TL 16, 37–50.

Aitken, M.J., 1985. Thermoluminescence dating. Academic press, London, 359 p.

Aitken, M.J., 1998. An introduction to optical dating. Oxford University Press, Oxford, 280 p.

Anechitei-Deacu, V., Timar-Gabor, A., Constantin, D., Trandafir-Antohi, O., del valle, L., Fornós, J.J., Gómez-Pujol, L., Wintle, A.G., 2018a. Assessing the maximum limit of sar-osl dating using quartz of different grain sizes. Geochronometria, accepted for publication.

Anechitei-Deacu, V., Timar-Gabor, A., Thomsen, K., Buylaert, J.-P., Jain, M., Bailey, M., Murray, A.S., 2018b. Single and multi-grain OSL investigations in the high dose range using coarse quartz. Radiation Measurements, in press, corrected proof.

Bøtter-Jensen, L., Thomsen, K.J., Jain, M., 2010. Review of optically stimulated luminescence (OSL) instrumental developments for retrospective dosimetry. Radiation Measurements 45, 253-257.

Buylaert, J.P., Murray, A.S., Vandenberghe, D., Vriend, M., De Corte, F., Van den haute, P., 2008. Optical dating of Chinese loess using sand-sized quartz: Establishing a time frame for Late Pleistocene climate changes in the western part of the Chinese Loess Plateau. Quaternary Geochronology 3, 99-113.

Buylaert, J.-P., Vandenberghe D., Murray, A.S., Huot, S, De Corte, F., Van den Haute, P., 2007. Luminescence dating of old (>70 ka) Chinese loess: A comparison of single-aliquot OSL and IRSL techniques. Quaternary Geochronology 2, 9-14.

Constantin, D., Begy, R., Vasiliniuc, S., Panaiotu, C., Necula, C., Codrea, V., Timar-Gabor, A., 2014. High-resolution OSL dating of the Costinești section (Dobrega, SE Romania) using fine and coarse quartz. Quaternary International 334-335, 20-29.

Constantin, D., Camenita, A., Panaiotu, C., Necula, C., Codrea, V., Timar-Gabor, A., 2015a. Fine and coarse-quartz SAR-OSL dating of Last Glacial loess in Southern Romania. Quaternary

International 357, 33-43.

del Valle, L., Gomez-Pujol, L., Fornos, J.-J., Timar-Gabor, A., Anechitei-Deacu, V., Pomar, F., 2016. Middle to Late Pleistocene dunefields in rocky coast settings at Cala Xuclar (Eivissa, Western Mediterranean): Recognition, architecture and luminescence chronology. Quaternary International 407, 4-13.

Dodonov, A.E., Zhou, L.P., Markova, A.K., Tchepalyga, A.L., Trubikhina, V.M., Aleksandrovski A.L., Simakova A.N., 2006. Middle–Upper Pleistocene bio-climatic and magnetic records of the Northern Black Sea Coastal Area. Quaternary International 149, 44-54.

Duller, G.A.T., 2003. Distinguishing quartz and feldspar in single grain luminescence measurements. Radiation Measurements 37, 161-165.

Duller, G.A.T., 2006. Single grain optical dating of glacigenic deposits. Quaternary Geochronology 1, 296–304.

Duval, M. and Guilarte, V., 2015. ESR dosimetry of optically bleached quartz grains extracted from Plio-Quaternary sediment: Evaluating some key aspects of the ESR signals associated to the Ti-centers. Radiation Measurements 78, 28-41.

Fornós, J.J., Clemmensen, L.B., Gómez-Pujol, L., Murray, A.S., 2009. Late Pleistocene carbonate aeolianites on Mallorca, Western Mediterranean: a luminescence chronology. Quaternary Science Reviews 28, 2697–2709.

Frechen, M., Schweitzer, U., Zander, A., 1996. Improvements in sample preparation for the fine grain technique. Ancient TL 14, 15–17.

Huntley, D.J., Godfrey-Smith, D.I., Thewalt, M.L.W., 1985. Optical dating of sediments. Nature 313, 105-107.

Huntley, D.J. and Prescott, J.R., 2001. Improved methodology and new thermoluminescence ages for the dune sequence in south-east South Australia. Quaternary Science Reviews 20, 687-699.

Lai, Z., 2010. Chronology and the upper dating limit for loess samples from Luochuan section in the Chinese Loess Plateau using quartz OSL SAR protocol. Journal of Asian Earth Sciences 37, 176-185.

Lang, A., Lindauer, S., Kuhn, R., Wagner, G.A., 1996. Procedures used for optically and infrared stimulated luminescence dating of sediments in Heidelberg. Ancient TL 14, 7–11.

Li, B., Roberts, R.G., Jacobs, Z., Li, S-H., 2015. Potential of establishing a global standardised growth curve (gSGC) for optical dating of quartz from sediments. Quaternary Geochronology 27, 94-104.

Lisiecki, L. and Raymo, M.E., 2005. A Pliocene–Pleistocene stack of 57 globally distributed benthic $\delta^{18}O$ records. Paleoceanography 20, PA1003.

Lowick, S.E. and Preusser, F., 2011. Investigating age underestimation in the high dose region of optically stimulated luminescence using fine grain quartz. Quaternary Geochronology 6, 33-41.

Lowick, S.E., Preusser, F., Pini, R., Ravazzi, C., 2010a. Underestimation of fine grain quartz OSL dating towards the Eemian: Comparison with palynostratigraphy from Azzano Decimo, northeastern Italy. Quaternary Geochronology 5, 583-590.

Lowick, S.E., Preusser, F., Wintle, A.G., 2010b. Investigating quartz optically stimulated luminescence dose–response curves at high doses. Radiation Measurements 45, 975-984.

Karátson, D., Wulf, S., Veres, D., Magyari, E.K., Gertisser, R., Timar-Gabor, A., Novothny, Á., Telbisz., T., Szalai, Z., Anechitei-Deacu, V., Appelt, O., Bormann, M., Jánosi, Cs., Hubay, K., Schäbitz, F., 2016. The latest explosive eruptions of Ciomadul (Csomád) volcano, East Carpathians — A tephrostratigraphic approach for the 51–29 ka BP time interval. Journal of Volcanology and Geothermal Research 319, 29-51.

Murray, A.S., Buylaert, J.-P., Henriksen, M., Svendsen, J.-I., Mangerud, J., 2008. Testing the reliability of quartz OSL ages beyond the Eemian. Radiation Measurements 43, 776-780.

Murray, A.S. and Olley, J.M., 2002. Precision and accuracy in the optically stimulated luminescence dating of sedimentary quartz: a status review. Geochronometria 21, 1-16.

Murray, A.S., Svendsen, J.I., Mangerud, J., Astakhov, V.I., 2007. Quartz OSL age of an Eemian site on the Sula River, Northern Russia. Quaternary Geochronology 2, 107-109.

Murray, A.S. and Wintle, A.G., 2000. Luminescence dating of quartz using an improved single-aliquot regenerative-dose protocol. Radiation Measurements 32, 57–73.

Murray, A.S. and Wintle, A.G., 2003. The single aliquot regenerative dose protocol: potential for improvements in reliability. Radiation Measurements 37, 377–381.

Pawley, S.M., Bailey, R.M., Rose, J., Moorlock, B.S.P., Hamblin, R.J.O., Booth, S.J., Lee, J.R., 2008. Age limits on Middle Pleistocene glacial sediments from OSL dating, north Norfolk, UK. Quaternary Science Reviews 27, 1363-1377.

Prescott, J.R., Huntley, D.J., Hutton, J.T., 1993. Estimation of equivalent dose in thermoluminescence dating - the Australian slide method. Ancient TL 11, 1-5.

Prescott, J.R. and Hutton, J.T., 1994. Cosmic ray contributions to dose rates for luminescence and ESR dating: Large depths and long term variations. Radiation Measurements 23, 497–500.

Roberts, H.M. and Duller, G.A.T., 2004. Standardised growth curves for optical dating of sediment using multiple-grain aliquots. Radiation Measurements 38, 241-252.

Roberts, H. and Wintle, A.G., 2001. Equivalent dose determinations for polymineralic fine-grains using the SAR protocol: application to a Holocene sequence of the Chinese Loess Plateau. Quaternary Science Reviews 20, 859-863.

Shackleton, N.J., 2000. The 100,000-year ice age cycle identified and found to lag temperature, carbon dioxide, and orbital eccentricity. Science 289, 1897–1902.

Singarayer, J.S. and Bailey, R.M., 2004. Component-resolved bleaching spectra of quartz optically stimulated luminescence: preliminary results and implications for dating. Radiation Measurements 38, 111–118.

Thomsen, K.J., Murray, A.S., Buylaert, J.P, Jain, M., Hansen, J.H., Aubry, T., 2016. Testing single-grain quartz OSL methods using sediment samples with independent age control from the Bordes-Fitte rockshelter (Roches d'Abilly site, Central France). Quaternary Geochronology 31, 77-96.

Timar, A., Vandenberghe, D., Panaiotu, E.C., Panaiotu, C.G., Necula, C., Cosma, C., Van den haute, P., 2010. Optical dating of Romanian loess using fine-grained quartz. Quaternary Geochronology 5, 143-148.

Timar-Gabor, A., Buylaert, J.-P., Guralnik, B., Trandafir-Antohi, O., Constantin, D., Anechitei-Deacu, V., Jain, M., Murray, A.S., Porat, N., Hao, Q., Wintle, A.G., 2017. On the importance of grain size in luminescence dating using quartz. Radiation Measurements 106, 464-471.

Timar-Gabor, A., Constantin, D., Buylaert, J.P., Jain, M., Murray, A.S., Wintle, A.G., 2015b. Fundamental investigations of natural and laboratory generated SAR dose response curves for quartz OSL in the high dose range. Radiation Measurements 81, 150-156.

Timar-Gabor, A., Constantin, D., Marković, S.B., Jain, M., 2015a. Extending the area of investigation of fine versus coarse quartz optical ages from the Lower Danube to the Carpathian Basin. Quaternary International 388, 168-176.

Timar-Gabor, A., Vandenberghe, D.A.G., Vasiliniuc, S., Panaiotu, C.E., Panaiotu, C.G., Dimofte, D., Cosma, C., 2011. Optical dating of Romanian loess: a comparison between sand-sized and silt-sized quartz. Quaternary International 240, 62-70.

Timar-Gabor, A., Vasiliniuc, S., Vandenberghe, D.A.G., Cosma, C., Wintle, A.G., 2012. Investigations on the reliability of SAR-OSL equivalent doses obtained for quartz samples displaying dose response curves with more than one component. Radiation Measurements 47, 740-745.

Timar-Gabor, A. and Wintle, A.G., 2013. On natural and laboratory generated dose response curves for quartz of different grain sizes from Romanian loess. Quaternary Geochronology 18, 34-40.

Toyoda, S. and Falguères, C., 2003. The method to represent the ESR signal intensity of the aluminium hole center in quartz for the purpose of dating. Advances in ESR applications 20, 7-10.

Tsatskin, A., Heller, F., Hailwood, E.A., Gendler, T.S., Hus, J., Montgomery, P., Sartori, M., Virina, E.I., 1998. Pedosedimentary division, rock magnetism and chronology of the loess/paleosol sequence at Roxolany (Ukraine). Palaeogeography, Palaeoclimatology, Palaeoecology, 143, 111-133.

Vandenberghe, D., De Corte, F., Buylaert, J.-P., Kučera, J., Van den haute, P., 2008. On the internal radioactivity in quartz. Radiation Measurements 43, 771 – 775.

Veres, D., Tecsa, V., Gerasimenko, N., Zeeden, C., Constantin, D., Hambach, U., Timar-Gabor, A. OSL dating constraints for a key Middle-to-Late Pleistocene loess-paleosol sequence in Eastern Europe (Stayky, Ukraine). Quaternary Science Reviews, submitted.

Wintle, A.G. and Murray, A.S., 2006. A review of quartz optically stimulated luminescence characteristics and their relevance in single-aliquot regeneration dating protocols. Radiation measurements 41, 369-391.